

Article

Regulation of Response Properties and Operating Range of the AFD Thermosensory Neurons by cGMP Signaling

Sara M. Wasserman,^{1,2} Matthew Beverly,¹ Harold W. Bell,¹ and Piali Sengupta^{1,*}

¹Department of Biology and National Center for Behavioral Genomics, Brandeis University, Waltham, MA 02454, USA

Summary

Background: The neuronal mechanisms that encode specific stimulus features in order to elicit defined behavioral responses are poorly understood. *C. elegans* forms a memory of its cultivation temperature (T_c) and exhibits distinct behaviors in different temperature ranges relative to T_c . In particular, *C. elegans* tracks isotherms only in a narrow temperature band near T_c . T_c memory is in part encoded by the threshold of responsiveness (T_{AFD}^*) of the AFD thermosensory neuron pair to temperature stimuli. However, because AFD thermosensory responses appear to be similar at all examined temperatures above T_{AFD}^* , the mechanisms that generate specific behaviors in defined temperature ranges remain to be determined.

Results: Here, we show that the AFD neurons respond to the sinusoidal variations in thermal stimuli followed by animals during isothermal tracking (IT) behavior only in a narrow temperature range near T_c . We find that mutations in the AFD-expressed *gcy-8* receptor guanylyl cyclase (rGC) gene result in defects in the execution of IT behavior and are associated with defects in the responses of the AFD neurons to oscillating thermal stimuli. In contrast, mutations in the *gcy-18* or *gcy-23* rGCs alter the temperature range in which IT behavior is exhibited. Alteration of intracellular cGMP levels via rGC mutations or addition of cGMP analogs shift the lower and upper ranges of the temperature range of IT behavior in part via alteration in T_{AFD}^* .

Conclusions: Our observations provide insights into the mechanisms by which a single sensory neuron type encodes features of a given stimulus to generate different behaviors in defined zones.

Introduction

Animals exhibit defined behaviors in response to specific aspects of a given sensory stimulus including its temporal dynamics, magnitude of change, or absolute value. Stimulus features could be encoded by peripheral sensory neurons with defined operating ranges [1–3] or by filtering and integration in neuronal networks [4, 5]. Much remains to be understood regarding the mechanisms by which specific stimulus features are represented in neuronal responses in both the peripheral and central nervous system.

C. elegans thermosensation provides an excellent system in which to explore the mechanisms underlying sensory neuron response properties. Within its physiological temperature

range, *C. elegans* exhibits different behaviors in different temperature ranges relative to its cultivation temperature (T_c) [6, 7] (Figure 1A). In a narrow temperature band near T_c , *C. elegans* tracks isotherms (isothermal tracking [IT]), whereas at higher temperatures, *C. elegans* exhibits negative thermotaxis [6–9] (Figure 1A). T_c memory is plastic and can be reset upon cultivation of worms at different temperatures [6, 10]. Thus, the *C. elegans* nervous system encodes a memory of T_c and compares the ambient temperature to this memory in order to direct specific behaviors in defined temperature bands within a broad temperature range.

The AFD sensory neuron pair is a major thermosensory neuron type in *C. elegans* [7]. Physical ablation of the AFD neurons abolishes IT behavior and severely affects negative thermotaxis [7, 11]. T_c memory appears to be partly stored in the AFD neurons as a threshold (referred to as T_{AFD}^*), above which these neurons exhibit thermosensory responses (Figures 1B and 1C) [10, 12–14]. However, the responses of the AFD neurons to examined thermal stimuli appear to be similar at all temperatures above T_{AFD}^* (Figures 1B and 1C) [12, 14, 15], raising the question of how different behaviors are elicited in different temperature ranges relative to T_c .

Thermosensory signal transduction in the AFD neurons is mediated via cGMP signaling. Animals mutant for the TAX-2 and TAX-4 cGMP-gated channels or triply mutant for the GCY-8, GCY-18, and GCY-23 receptor guanylyl cyclases (rGCs) are atactic and fail to exhibit temperature-induced currents in the AFD neurons [6, 7, 13, 15]. These rGCs are expressed specifically or selectively in the AFD neurons and are localized to their sensory receptive endings [16–18]. However, the roles of individual rGCs in the regulation of IT behavior have not been examined. In addition, whether mutations in single *gcy* genes affect specific aspects of AFD thermosensitivity has not been investigated.

Here we show that the AFD neurons respond robustly to thermal stimuli that mimic the thermosensory inputs animals encounter when tracking isotherms, but that they do so only in the range in which IT behavior is exhibited. We find that GCY-8, but not other rGCs, regulates the ability of the AFD neurons to respond to this stimulus and execute IT. Alterations in cGMP signaling shift the lower and upper bounds of the range in which the AFD neurons are able to respond to this stimulus and elicit IT behavior. Our results indicate that individual rGCs regulate different aspects of AFD thermosensory functions and that precise regulation of intracellular cGMP signaling regulates the temperature range in which the AFD neurons are able to respond to specific thermal stimuli. These observations suggest a mechanism by which regulation of AFD neuronal activity contributes to the generation of different behaviors in distinct temperature zones above T_c .

Results

Animals Lacking the AFD Neurons, or Mutant for the *tax-4* Cyclic Nucleotide-Gated Gene, Fail to Initiate and Maintain Isothermal Tracks

Mutations in the *tax-4* cyclic nucleotide-gated (CNG) channel have been shown to abolish AFD thermosensitivity and IT

*Correspondence: sengupta@brandeis.edu

²Present address: Howard Hughes Medical Institute, Department of Integrative Biology and Physiology, University of California, Los Angeles, Los Angeles, CA 90095, USA

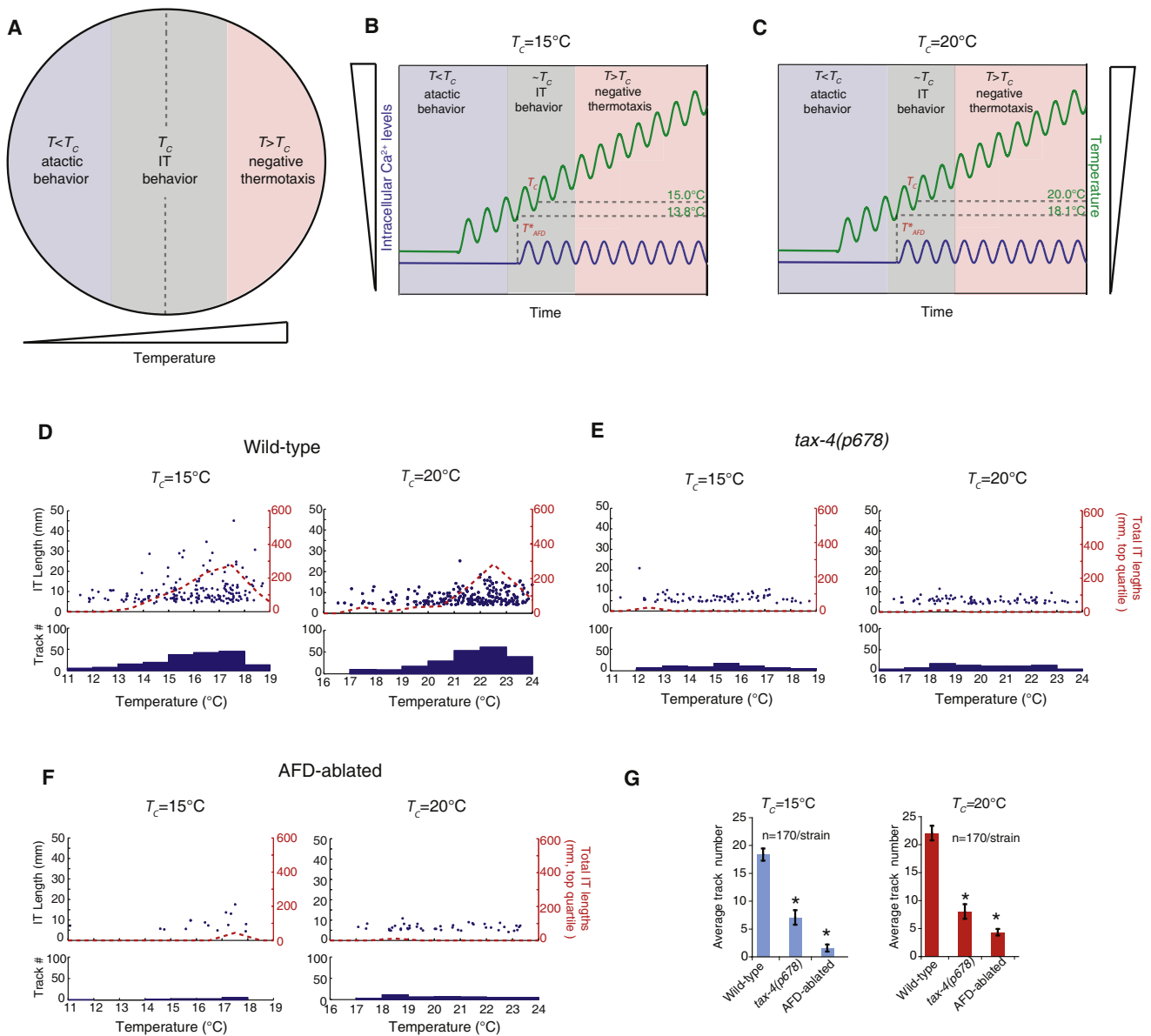


Figure 1. The AFD Thermosensory Neurons and TAX-4 CNG Channel Are Required to Initiate and Maintain Isothermal Tracks

(A) Diagrammatic representation of behaviors exhibited in different temperature ranges relative to T_c . (B and C) Diagrammatic representations of intracellular calcium (Ca^{2+}) changes (blue lines) in the AFD neurons in response to an upward oscillating temperature stimulus (green lines). T_c is $15^\circ C$ (B) or $20^\circ C$ (C). T_{AFD}^* refers to the temperature at which intracellular Ca^{2+} dynamics are first observed in the AFD neurons. Note that T_{AFD}^* is altered in a T_c -dependent manner. Adapted from [12]. (D–F) Scatter plots of numbers and lengths of isothermal tracks (>3.6 mm; see Supplemental Experimental Procedures) exhibited by wild-type (D), *tax-4* (*p678*) (E), and AFD-ablated (F) animals (170 animals per strain) grown at the indicated T_c on a linear thermal gradient of $0.9^\circ C/cm$ steepness. The red dotted lines indicate the total lengths of isothermal tracks in the top quartile of all measured wild-type isothermal track lengths in the assay at the indicated temperatures (also see Supplemental Experimental Procedures). Histograms below indicate the total numbers of isothermal tracks at different temperatures. 10 independent assays ($n = 17$ animals each) were conducted for each genotype. See also Figure S1. (G) Average isothermal track numbers exhibited by animals of the indicated genotypes. Asterisk indicates values that are different from those of corresponding wild-type animals at $p < 0.05$ via one-way ANOVA followed by Dunnett’s posthoc test. Error bars are the SEM. The average from 10 independent assays ($n = 17$ animals each) for each genotype are shown.

behavior [6, 7, 13, 15]. We first determined whether the inability of *tax-4* mutants to track isotherms arises from defects in initiation and/or maintenance of IT behavior. Animals were grown at a T_c of $15^\circ C$ or $20^\circ C$ and placed on a $0.9^\circ C/cm$ linear thermal gradient that includes the temperatures at which IT behavior is expected. We quantified the numbers of tracks perpendicular to the direction of the gradient to obtain a measure of initiated

isothermal tracks, as well as isothermal track lengths to determine maintenance of IT behavior. Under our experimental conditions, the average length of an isothermal track on a plate in the absence of an imposed thermal gradient is ~ 3.6 mm (see Supplemental Experimental Procedures available online). Quantification of isothermal track numbers that were longer than 3.6 mm on a thermal gradient showed that wild-type

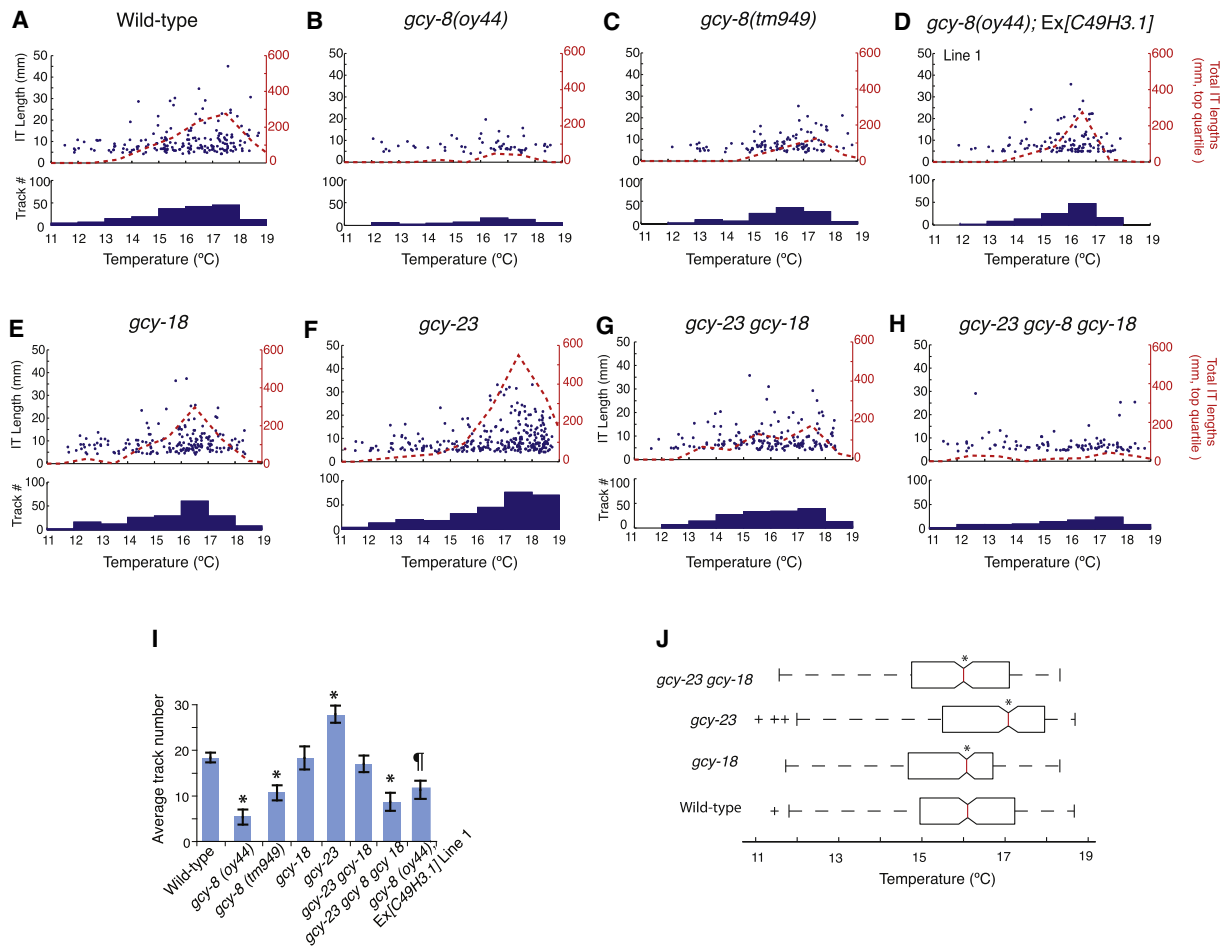


Figure 2. rGCs Regulate IT Behavior at $T_c = 15^\circ\text{C}$

(A–H) Scatter plots and histograms of numbers and lengths of isothermal tracks as described in the legend to Figure 1 exhibited by animals of the indicated genotypes grown at $T_c = 15^\circ\text{C}$. Data in (A) are from Figure 1D. Wild-type *gcy-8* genomic sequences present on the C49H3.1 cosmid were coinjected together with bacterial DNA in a complex array to generate two independent lines [41], and the responses of transgenic animals from one line are shown in (D). 10 independent assays ($n = 17$ animals each) were conducted for each genotype. See also Figures S1 and S2.

(I) Average isothermal track numbers exhibited by animals of the indicated genotypes on a $0.9^\circ\text{C}/\text{cm}$ gradient. Asterisk indicates values that are different from that of corresponding wild-type animals at $p < 0.05$ via one-way ANOVA followed by Dunnett’s posthoc test. Paragraph sign (§) indicates values that are different from those of *gcy-8(oy44)* mutants at $p < 0.05$. Error bars are the SEM. Shown is the average of pooled results from 10 independent assays ($n = 17$ animals each) per genotype.

(J) Box-and-whisker plots of the temperature range on a linear thermal gradient in which isothermal tracks are exhibited. For this quantification, only mutants exhibiting track numbers similar to or greater than those exhibited by AFD-ablated animals were included. Boxes indicate the 25th (right boundary), 50th (median indicated by a red line), and 75th (left boundary) percentiles. Whiskers show the minimum and maximum temperatures. Outliers are indicated by plus symbols. Asterisk indicates distributions that are different from those of wild-type animals at $p < 0.05$ via the Kolmogorov-Smirnov test. $n = 170$ animals for each genotype; 10 independent assays each.

animals initiated more tracks in a temperature band near T_c (Figure 1D). Moreover, in the presence of a gradient, wild-type animals maintained movement along isotherms near T_c as evident from longer isothermal track lengths in this temperature band (Figure 1D).

In contrast, we found that the isothermal tracks initiated by *tax-4(p678)* mutants were evenly distributed across the gradient (Figure 1E). Moreover, *tax-4* mutants initiated fewer of these tracks overall (Figure 1G) and exhibited only rare longer tracks (Figure 1E). Because IT behavior requires forward movement and suppression of abrupt reorientation events or turns [8, 9], we confirmed that the tracking defects of *tax-4* mutants were not due to increased basal turning rates or changes in forward movement velocity (Figure S1). Consistent with a major role of the AFD neurons in regulating IT behavior,

animals in which the AFD neurons had been genetically ablated (generous gift from M. Goodman, Stanford University) also initiated significantly fewer isothermal tracks (Figures 1F and 1G) that were not maintained (Figure 1F). These results indicate that the AFD neurons and TAX-4 CNG channel are required to both initiate and maintain isothermal tracks.

The GCY-8 rGC Is Required for Isothermal Tracking Behavior

We next determined whether one or more of the AFD-expressed GCY-8, GCY-18, or GCY-23 rGCs regulate IT behavior. We first confirmed that all examined *gcy* mutants exhibited normal locomotion and turning rates (Figure S1). We found that animals carrying two independent alleles of *gcy-8* (Figure S2) exhibited significant defects in IT behavior. *gcy-8(oy44)*, and to a lesser

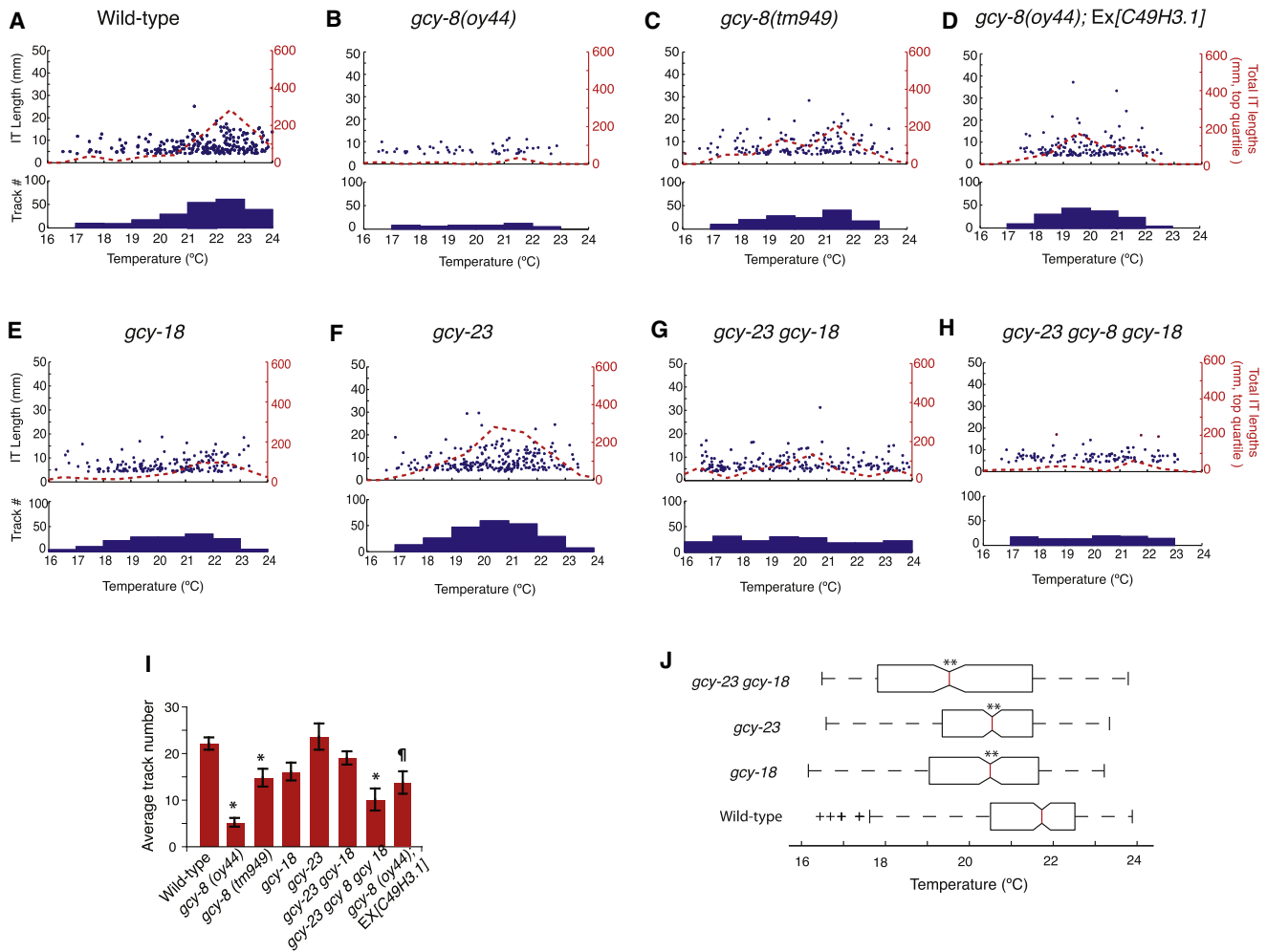


Figure 3. rGCs Regulate IT Behavior at $T_c = 20^\circ\text{C}$

(A–H) Scatter plots and histograms of numbers and lengths of isothermal tracks as described in the legend to Figure 1 exhibited by animals of the indicated genotypes grown at $T_c = 20^\circ\text{C}$. Data in (A) are from Figure 1D.

(I) Average isothermal track numbers exhibited by animals of the indicated genotypes on a $0.9^\circ\text{C}/\text{cm}$ gradient. Asterisk indicates values that are different from that of corresponding wild-type animals at $p < 0.05$ via one-way ANOVA followed by Dunnett's posthoc test. Paragraph sign (¶) indicates values that are different from those of *gcy-8(oy44)* mutants at $p < 0.05$. Error bars are the SEM. Shown is the average of pooled results from 10 independent assays ($n = 17$ animals each) per genotype.

(J) Box-and-whisker plots of the temperature range on a linear thermal gradient in which isothermal tracks are exhibited as described in the legend to Figure 2. Double asterisk indicates distributions that are different from those of wild-type animals at $p < 0.0001$ via the Kolmogorov-Smirnov test. $n = 170$ animals for each genotype; 10 independent assays each.

extent *gcy-8(tm949)*, mutants grown at either 15°C or 20°C showed defects in isothermal track maintenance as compared to wild-type animals (Figures 2A–2C and 3A–3C). These mutants also exhibited significantly fewer overall isothermal track numbers at both temperatures, with *gcy-8(tm949)* mutants exhibiting weaker defects than *gcy-8(oy44)* animals particularly at 20°C (Figures 2I and 3I). The tracking defects of *gcy-8(oy44)* mutants were partially rescued upon expression of low copy numbers of a cosmid containing wild-type *gcy-8* genomic sequences in one of two transgenic lines examined (Figures 2D, 2I, 3D, and 3I). *gcy-8(oy44)/gcy-8(tm949)* heterozygous animals also exhibited significant IT defects (data not shown).

In contrast, *gcy-18* mutants exhibited similar isothermal track numbers and lengths as wild-type animals when grown at either 15°C or 20°C (Figures 2E, 2I, 3E, and 3I). *gcy-23* mutants grown at 15°C but not at 20°C initiated a significantly larger number of isothermal tracks on a thermal gradient

(Figures 2F, 2I, 3F, and 3I) and also exhibited longer tracks (Figure 2F). However, the distribution of tracks exhibited by both *gcy-18* and *gcy-23* mutants on the gradient was distinct from that of wild-type animals (discussed further below). The phenotypes of *gcy-23 gcy-18* double-mutant animals resembled those of *gcy-18* mutants alone at both examined temperatures (Figures 2G, 2I, 3G, and 3I), whereas *gcy-23 gcy-8 gcy-18* triple-mutant animals exhibited strong defects in IT behavior at both temperatures resulting from defects in both initiation and maintenance of isothermal tracks (Figures 2H, 2I, 3H, and 3I). These results indicate that GCY-8 regulates the ability of the AFD neurons to execute IT behavior.

GCY-18 and GCY-23 rGCs Regulate the Temperature Range of Tracking

The temperature range in which animals track isotherms reflects the animals' memory of T_c [6, 7, 10]. Mutants that are

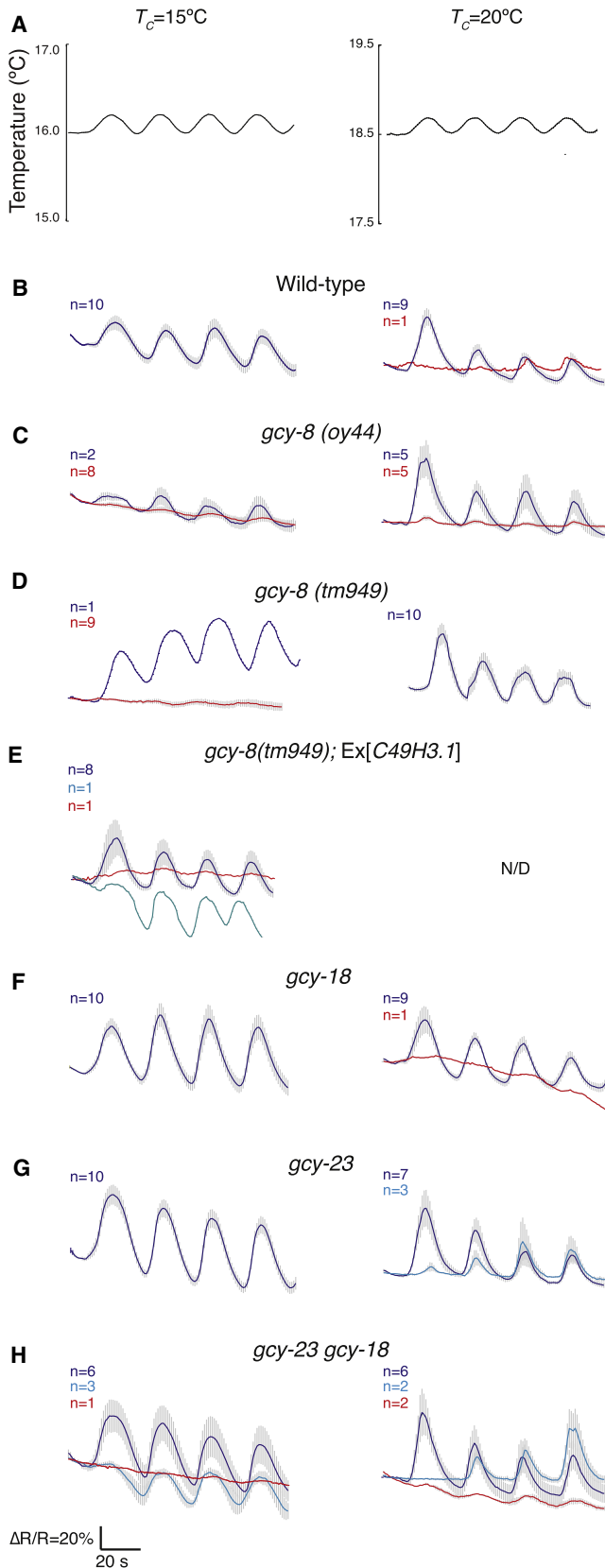


Figure 4. Intracellular Ca^{2+} Dynamics in the AFD Neurons in Response to Oscillating Thermal Stimuli

(A) Representative oscillatory temperature stimuli used at each T_c .

(B–H) Changes in average intracellular Ca^{2+} dynamics in cameleon YC3.60–

able to respond to oscillating temperature stimuli and track isotherms may nevertheless do so in a different temperature range if their T_c memory is distinct from that of wild-type animals. The distribution of isothermal tracks exhibited by *gcy-18* and *gcy-23* mutants appeared to be different from that of wild-type animals, so we quantified the temperature range in which these *gcy* mutants exhibited significant IT ability. We found that the distribution range of isothermal tracks in *gcy-18* mutants was shifted toward colder temperatures at both $T_c = 15^\circ\text{C}$ and $T_c = 20^\circ\text{C}$, with the shift being larger at $T_c = 20^\circ\text{C}$ (Figures 2J and 3J). However, whereas the distribution of isothermal tracks in *gcy-23* mutants was also shifted toward colder temperatures at $T_c = 20^\circ\text{C}$ (Figure 3J), the range was shifted to warmer temperatures at $T_c = 15^\circ\text{C}$ (Figure 2J). The range in *gcy-23 gcy-18* double mutants was not significantly different from that of *gcy-18* single mutants at $T_c = 15^\circ\text{C}$ (Figure 2J) but showed an additive effect at $T_c = 20^\circ\text{C}$ (Figure 3J). These results imply that whereas GCY-18 and GCY-23 are not essential for the execution of IT behavior, these rGCs play important roles in setting T_c memory.

Mutations in *gcy-8* Affect the Ability of the AFD Neurons to Respond to Oscillating Thermal Stimuli

IT behavior requires that animals be able to sense oscillating temperature stimuli around a reference temperature; the amplitude and frequency of the oscillating stimulus are dependent on the steepness of the gradient and the speed of the animals' sinusoidal movement [8, 9, 19]. The thermosensory responses of the AFD neurons have previously been shown to be bidirectional and adaptive [12, 14, 15], allowing animals to respond to the oscillatory temperature changes that the animal experiences while navigating a linear thermal gradient. We hypothesized that the failure of *gcy-8* mutants to track isotherms on steep gradients could arise from defects in the ability of the AFD neurons to respond to these rapidly oscillating temperature changes. To address this possibility, we expressed the genetically encoded ratiometric Ca^{2+} sensor YC3.60 cameleon [20, 21] in the AFD neurons under the *gcy-8* promoter and examined intracellular Ca^{2+} dynamics in response to sinusoidal variations in temperature.

We examined Ca^{2+} dynamics in response to oscillatory stimuli of 0.04 Hz frequency and 0.2°C amplitude centered around $\sim 16.1^\circ\text{C}$ and $\sim 18.6^\circ\text{C}$ for animals grown at 15°C and 20°C , respectively (Figure 4A). These stimuli correspond to temporal temperature variations of approximately 0.008°C/s , which is within the range of sensitivity of temporal sensory processing required for isothermal tracking [8]. The reference mean temperatures were chosen because they were above

expressing AFD neurons of animals of the indicated genotypes grown at $T_c = 15^\circ\text{C}$ (left) or $T_c = 20^\circ\text{C}$ (right). Sinusoidal stimuli had a frequency of 0.04 Hz and amplitudes of 0.2°C centered around 16.1°C (for $T_c = 15^\circ\text{C}$) or 18.6°C ($T_c = 20^\circ\text{C}$). Also see Figure S3B. In each panel, the average percentage change in phase-locked Ca^{2+} dynamics is shown in dark blue ($\Delta R = (R - R_0)/R_0$, where R is the fluorescence emission ratio and R_0 is the baseline). In red is shown the average percentage change in fluorescence ratio in nonresponding AFD neurons. Averages of the responses that initiated later or showed phase alterations are indicated in cyan. The number of AFD neurons in each category (phase-locked responses, delayed responses, or responses with altered phase, no responses) are indicated at the top left of each panel in the corresponding colors. Grayed out bands indicate ± 1 SEMs of the response. Statistical significances of proportions are indicated in Table 1. Example responses of individual AFD neurons in wild-type animals are shown in Figure S3A.

Table 1. Responses of AFD Neurons in *gcy* Mutants to Oscillating Temperature Stimuli

Stimulus Frequency (Hz)	Stimulus Amplitude (°C)	Stimulus Range (°C)	T_c	Strain	% AFD Neurons Exhibiting Phase-Locked Responses	% AFD Neurons Responding ^a	p Values ^b
0.04	0.2	16.0–16.2	15°C	wild-type	100	100	
				<i>gcy-8(oy44)</i>	20	20	<0.0001 ^c
				<i>gcy-8(tm949)</i>	10	10	<0.0001 ^c
				<i>gcy-8(tm949); Ex[C49H3.1]</i>	80	90	
				<i>gcy-18</i>	100	100	
				<i>gcy-23</i>	100	100	
				<i>gcy-23 gcy-18</i>	60	90	
0.04	0.2	18.5–18.7	20°C	wild-type	90	90	
				<i>gcy-8(oy44)</i>	50	50	= 0.05
				<i>gcy-8(tm949)</i>	100	100	
				<i>gcy-18</i>	90	90	
				<i>gcy-23</i>	70	100	
				<i>gcy-23 gcy-18</i>	60	80	
				wild-type	100	100	
0.04	0.5	16.0–16.5	15°C	wild-type	100	100	
				<i>gcy-8(oy44)</i>	20	20	<0.0001 ^c
				<i>gcy-18</i>	90	90	
				<i>gcy-23</i>	80	80	
				<i>gcy-23 gcy-18</i>	80	80	

n = 10 neurons (1 neuron/animal) for all conditions.

^a Includes neurons that exhibit both phase-locked responses as well as responses that are delayed or that are not phase-locked to the stimulus.

^b Compared to the percentage of responding AFD neurons in wild-type animals. Only p values that are significantly different at $p < 0.05$ are indicated. p values were determined with a χ^2 test of independence.

^c Compared to wild-type values under the same conditions.

the corresponding T^*_{AFD} and within the temperature range at which IT behavior is exhibited. Most if not all examined wild-type AFD neurons (90%–100%; n = 10 each) responded robustly to this stimulus at both temperatures and exhibited intracellular Ca^{2+} dynamics that were phase-locked onto the provided stimulus (Figure 4B, Table 1; Figure S3A). Because the ability of the AFD neurons to track oscillatory thermal stimuli is probably associated with their ability to direct IT behavior [12], we elected to quantify the number of AFD neurons exhibiting oscillatory responses in mutants regardless of response amplitude. In contrast to wild-type animals, only 10%–20% (n = 10 each) of the examined AFD neurons in *gcy-8(oy44)* and *gcy-8(tm949)* animals responded to the stimulus in animals grown at 15°C. Only 20% of the AFD neurons in *gcy-8* mutants also responded to oscillating stimuli of a larger amplitude of 0.5°C with a similar stimulus frequency (Table 1; Figure S3B). Whereas 50% of the AFD neurons in *gcy-8(oy44)* mutant animals responded when grown at 20°C, all AFD neurons of *gcy-8(tm949)* mutant animals responded at 20°C (Figures 4C and 4D, Table 1), consistent with weaker isothermal tracking behavioral defects exhibited by *gcy-8(tm949)* mutants at this temperature (Figure 3). We verified that the observed defects were due to mutations in *gcy-8* by confirming that the defects in AFD Ca^{2+} dynamics in *gcy-8(tm949)* at $T_c = 15^\circ C$ mutants could be rescued upon expression of wild-type *gcy-8* sequences (Figure 4E).

Both *gcy-18* and *gcy-23* mutants retained the ability to respond to the oscillating stimuli with 0.2°C amplitude at either T_c examined (Figures 4F and 4G, Table 1), consistent with their ability to track isotherms when grown at these temperatures. We noted that a subset of the neurons in *gcy-23* mutants appeared to initiate responses later for reasons that are presently unclear (Figure 4G, Table 1). The majority of AFD neurons in *gcy-23 gcy-18* mutants also exhibited Ca^{2+} responses, with a small subset exhibiting delays in response initiation (Figure 4H, Table 1). Together, these results indicate that mutations in *gcy-8*, but not in *gcy-18* and *gcy-23*, affect the ability

of the AFD neurons to respond to oscillating temperature stimuli centered around a mean temperature.

cGMP Levels Regulate Setting of the Cultivation Temperature Memory

As indicated above, although *gcy-18* and *gcy-23* mutants retained the ability to track isotherms, they did so in a distinct temperature range, suggesting that their T_c memory was altered. To determine whether altered T_c memory correlated with changes in their T^*_{AFD} , we provided animals with thermal oscillations superimposed on warming ramps and quantified the average temperature at which intracellular Ca^{2+} transients are first observed (Figures 1B and 1C). Wild-type AFD neurons showed onset of Ca^{2+} changes at an average of 13.8°C or 18°C in animals grown at 15°C or 20°C, respectively (Figures 5A and 5B; Figure S4) [10, 12, 13]. Consistent with a larger downward shift in T_c memory of *gcy-18* mutants grown at 20°C, the T^*_{AFD} in their AFD neurons was also significantly lower, although no significant changes were observed at $T_c = 15^\circ C$ (Figures 5A and 5B). However, T^*_{AFD} of *gcy-23* mutants was not altered at either temperature (Figures 5A and 5B), suggesting that the altered T_c in these animals may reflect changes in the threshold of AFD synaptic output but not in its sensory response [10]. *gcy-23 gcy-18* double mutants exhibited T^*_{AFD} that was significantly lower than that exhibited by *gcy-18* or *gcy-23* mutants alone at $T_c = 20^\circ C$, reflecting the markedly lower T_c memory at this temperature as measured behaviorally (Figure 5B).

Although defects in tracking behavior precluded accurate measurements of T_c memory via behavioral assays in *gcy-8* mutants, the AFD neurons in these animals responded robustly to oscillating stimuli superimposed on an upward linear ramp (Figure S4), allowing quantification of T^*_{AFD} . Interestingly, T^*_{AFD} of *gcy-8* mutants was also lower than wild-type T^*_{AFD} in animals grown at either temperature (Figures 5A and 5B), indicating that mutations in AFD-expressed rGC genes regulate the range of IT behavior in part via regulation of T^*_{AFD} .

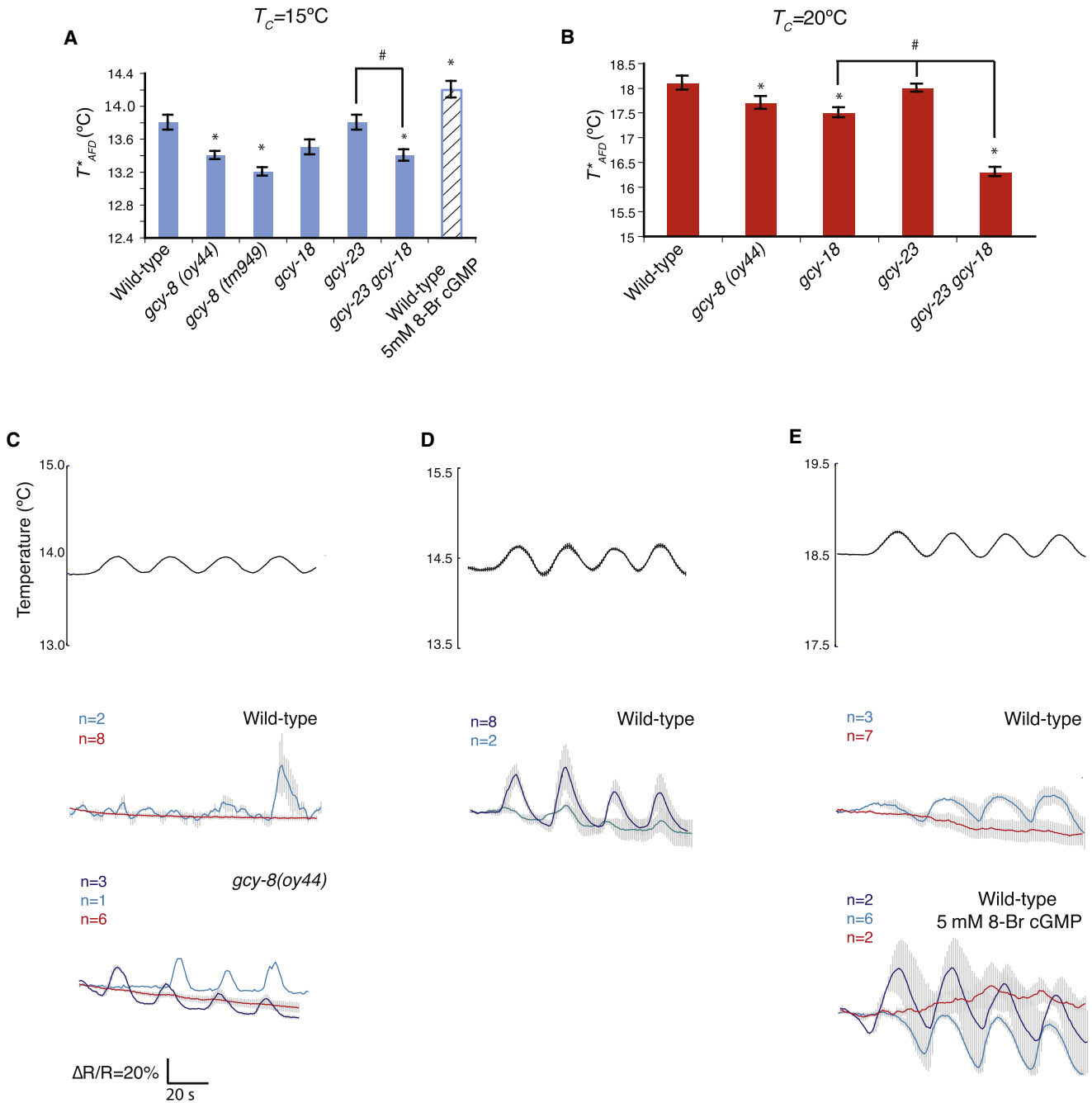


Figure 5. cGMP Signaling Sets the Lower and Upper Bounds of the Temperature Range in which AFD Neurons Respond to Oscillating Stimuli (A and B) Average temperatures at which AFD neurons in animals grown at 15°C (A) or 20°C (B) first exhibit changes in intracellular Ca^{2+} levels in response to a warming oscillating temperature ramp (see Figure S4 for representative temperature stimuli and response). Wild-type animals were grown overnight in the presence of 5 mM 8-Br-cGMP and T^*_{AFD} was quantified in the absence of added analog. $n = 9-10$ neurons each. Asterisk indicates values that are different from that of wild-type animals via one-way ANOVA and Tukey's HSD posthoc test at $p < 0.05$. Hatch mark (#) indicates values of *gcy-18* or *gcy-23* mutants that are different from that of the *gcy-23 gcy-18* double mutant at $p < 0.05$. Error bars are SEM. (C-E) Responses of animals of the indicated genotypes cultivated at 15°C in the absence or presence of 5 mM 8-Br-cGMP to oscillating temperature stimuli centered around ~13.9°C (C), 14.5°C (D), or 18.6°C (E). Phase-locked responses are shown in dark blue, no responses in red, and responses with delayed or altered phases in cyan. Numbers in panel in the corresponding colors indicate the number of neurons in each category. Statistical significances of proportions are shown in Table 2. Grayed out bands indicate \pm SEMs of the response.

Because mutations in *gcy* genes are expected to alter intracellular cGMP levels, we next quantified T^*_{AFD} in wild-type animals grown in the presence of the nonhydrolyzable cGMP analog 8-Br-cGMP. Addition of this analog to the cultivation plates raised T^*_{AFD} (Figure 5A). We could not measure their T_c memory

behaviorally because of general deficits in locomotory behavior in the presence of this analog (data not shown). Previous observations have also suggested that increased levels of cGMP may shift T_c memory toward higher temperatures [16]. Together, these observations strongly suggest that alterations in

intracellular cGMP signaling via mutations in rGC genes or by the addition of cGMP analogs alter T_c memory at least in part via altering the threshold of AFD responsiveness.

cGMP Levels Set the Upper Bound of the Response Range of the AFD Neurons to Oscillating Temperature Stimuli

The lower bound of the temperature range in which animals exhibit IT behavior is partly set by T_{AFD}^* [12, 13], which in turn appears to be regulated by intracellular cGMP signaling. However, how the upper bound is set is unclear. It is possible that the AFD neurons are able to respond to oscillating temperature stimuli only within the defined temperature range in which IT behavior is exhibited, although this possibility has not been tested experimentally. We hypothesized that the upper bound of the range in which IT behavior is exhibited at a given T_c is also set by intracellular cGMP signaling, thereby defining an operating range of the AFD neurons to this stimulus.

To test this notion, we examined the Ca^{2+} responses of wild-type AFD neurons to an oscillating stimulus of 0.04 Hz frequency and 0.2°C amplitude centered around ~13.9°C, ~14.5°C, and ~18.6°C for animals grown at 15°C and compared these responses to their responses at 16°C (Figures 5C–5E, Table 2). Only 20%–30% of wild-type AFD neurons exhibited responses at either the low or the high temperature extremes, compared to a 100% response rate at 14.5°C or 16°C (Figures 5C–5E, compare with Figure 4B, Table 2), providing a first indication of a defined operating response range of the AFD neurons to this stimulus. The T_{AFD}^* of *gcy-8* mutants is lower than that of wild-type; we therefore considered the possibility that the operating range of *gcy-8* mutants may be shifted toward lower temperatures. However, *gcy-8* (*oy44*) mutants continued to exhibit significant defects in response to an oscillating stimulus centered around 13.9°C (Figure 5C). Since addition of 8-Br-cGMP raised T_{AFD}^* (Figure 5A), we next determined whether the upper bound of the response was also shifted concomitantly. We found that growth of wild-type animals in the presence of 8-Br-cGMP resulted in a more robust response at the higher temperature, with 80% of neurons responding albeit with alterations in phase (Figure 5E, Table 2). These results imply that intracellular cGMP signaling sets both the upper and lower bound of responsiveness to oscillating stimuli, thereby defining the temperature range for IT behavior.

Discussion

We have shown that mutations in individual rGC genes or growth in the presence of a cGMP analog regulate the ability of the AFD neurons to respond to oscillating temperature stimuli and modulate the temperature range in which the AFD neurons are able to respond to these stimuli. Our results imply that differential responses of the AFD neurons in different temperature zones contribute to the generation of distinct thermosensory navigation behaviors on a linear thermal gradient.

Individual rGC Genes Regulate Different Aspects of AFD Neuron Function

Loss-of-function mutations in *gcy-8* result in marked IT behavioral defects resulting from defects in both isothermal track initiation and maintenance. Correspondingly, the AFD neurons of *gcy-8* mutants exhibit defects in their ability to respond to oscillating temperature stimuli centered around T_c . In contrast, *gcy-18* and *gcy-23* mutants retain the ability to track isotherms

and the AFD neurons in these mutants continue to respond to these oscillating stimuli. However, *gcy-18* and *gcy-23* mutants track isotherms in distinct temperature zones, and both *gcy-18* and *gcy-8* mutants exhibit altered T_{AFD}^* . Thus, although all three rGC genes play roles in regulating the temperature range in which IT behavior can be exhibited, only *gcy-8* regulates the ability of the AFD neurons to execute IT behavior.

Genes encoding these three rGCs are linked on LG IV and share extensive sequence homology [16]. Phylogenetic analyses indicate that these proteins belong to a larger nematode-specific clade and are likely to have arisen via gene duplication [22]. However, their functions in the AFD neurons appear to have diverged. GCY-18 and GCY-23 do not have completely redundant functions, because the majority of phenotypes of the *gcy-23 gcy-18* double mutants are not significantly stronger than those of *gcy-18* single mutants alone. Mutations in *gcy-23* affect the temperature range of IT behavior without affecting T_{AFD}^* , suggesting that the changes in cGMP signaling in *gcy-23* mutants may be sufficient to alter the threshold of AFD synaptic output but not that of sensory responses. It is possible that GCY-18 and GCY-23 are required under other conditions that require AFD function [16] and contribute to other phenotypes including regulation of lifespan [23, 24] and systemic heat shock responses [25]. The AFD neurons have been reported to express additional rGCs [16, 18], which may further contribute to AFD functional complexity. Similar complexity in rGC functions has been reported in the ASE chemosensory neurons in *C. elegans* that express >10 rGC genes [18, 26].

cGMP Signaling Probably Sets the Lower and Upper Bound of AFD Response Range

Our results indicate that the AFD neurons are able to respond to oscillating temperature stimuli only within a narrow temperature zone relative to T_{AFD}^* . The lower and upper bounds of this response range are altered in rGC mutants and upon growth in the presence of 8-Br-cGMP, suggesting that reduction or increase in cGMP signaling results in a lowering or raising of T_{AFD}^* , respectively, with corresponding shifts in the upper bounds.

A decrease or increase in intracellular cGMP signaling requires a lower or higher temperature, respectively, to initiate AFD neuronal activity at a given T_c . A simple possibility is that the enzymatic activity of the rGCs themselves is temperature dependent and that the TAX-2/4 CNG channels adapt to prevailing cGMP signaling at a given T_c . Indeed, *C. elegans* guanylyl cyclases have been reported to exhibit temperature-dependent activity [17, 27]. Thus, in AFD neurons with decreased cGMP signaling resulting from loss-of-function mutations in one or more rGCs, the CNG channels may have adapted to lower cGMP concentrations at T_c . Hence, the increase in intracellular cGMP upon a small rise in temperature may be sufficient to open the channels resulting in a lower T_{AFD}^* than in wild-type AFD neurons. Conversely, if the CNG channels are adapted to high cGMP levels at T_c , higher temperatures may be needed to generate sufficient cGMP in order to enable channel opening, leading to a higher T_{AFD}^* . CNG channel opening and sensitivity are known to be regulated by diverse mechanisms including phosphorylation, binding of Ca^{2+} /calmodulin, and phospholipids [28–35]. One or more of these mechanisms may contribute to the adaptation of the channels at T_c . Additional mechanisms such as changes in expression of the rGCs may also play a role in setting the T_{AFD}^* [36].

Table 2. cGMP Signaling Modulates the Response Range of the AFD Neurons

Stimulus Frequency (Hz)	Stimulus Amplitude (°C)	Stimulus Range (°C)	T_c	Strain	% AFD Neurons Exhibiting Phase-Locked Responses	% AFD Neurons Responding ^a	p Values ^b
0.04	0.2	13.8–14.0	15°C	wild-type	0	20	<0.0001 ^c
0.04	0.2	14.4–14.6	15°C	wild-type	80	100	
0.04	0.2	16.0–16.2	15°C	wild-type	100	100	
0.04	0.2	18.5–18.7	15°C	wild-type	0	30	<0.005 ^c
				wild-type 5 mM 8-Br cGMP	20	80	<0.05 ^d

n = 10 neurons (1 neuron/animal) for all conditions.

^a Includes all responding neurons.

^b p values were determined with a χ^2 test of independence. Only p values that are significantly different at $p < 0.05$ are indicated.

^c Compared to the percentage of responding AFD neurons in wild-type animals exposed to the same stimulus at 16.0°C–16.2°C and $T_c = 15^\circ\text{C}$.

^d Compared to the percentage of responding AFD neurons in wild-type animals exposed to the same stimulus at 18.5°C–18.7°C in the absence of exposure to 8-Br-cGMP.

Why do the AFD neurons respond to oscillating stimuli only at temperatures close to T_{AFD}^* ? One possibility is that in this range, the concentration of cGMP and the number of open channels are optimal to permit a high degree of sensitivity to rapid temperature changes. At higher temperatures, more channels may be open, decreasing the gain, which may in turn set the upper bound by decreasing neuronal sensitivity. Loss of GCY-8 affects the ability of the AFD neurons to respond to rapid temperature changes around T_c , suggesting that GCY-8, but not GCY-18 or GCY-23, plays an important role in rapid temperature-dependent cGMP production around T_c . However, *gcy-8* mutants respond normally to upward oscillating ramps, perhaps because of involvement of other rGCs when temperatures begin to rise. It is important to note, however, that current experiments are unable to distinguish between temperature-dependent regulation of rGCs versus phosphodiesterases.

Regardless of the exact mechanism, adaptation to T_c and modulation of cGMP signaling allows the AFD neurons to both maintain a high degree of sensitivity in the required temperature range and retain the ability to respond to a broad temperature range. This is reminiscent of mechanisms of peripheral and central gain control in sensory systems such as in vision and audition that permit both sensitivity and accuracy in sensory responses across a wide dynamic range [37, 38].

Different Thermosensory Neuron Response Properties Evoke Specific Behaviors in Defined Thermal Zones

We and others previously showed that the AWC polymodal sensory neurons exhibit different responses at temperatures near, above, or below T_c [39, 40]. We now find that the AFD neurons are also differentially responsive to oscillating temperature stimuli in the temperature range at which IT behavior is exhibited. Thus, the temperature range-specific responses of the AFD neurons and AWC neurons permit IT behavior in a defined temperature zone. Integration of differential responses from multiple sensory neurons under specific conditions may increase the robustness and precision of the thermosensory behavioral response.

Thermotaxis in *C. elegans* is a remarkably complex experience-dependent behavior. Identification and characterization of the molecular mechanisms underlying sensory neuron response properties to distinct features of thermal stimuli may now permit analyses of how these patterns are integrated

and translated through the circuit into precise changes in locomotor output.

Experimental Procedures

IT behavioral assays and Ca^{2+} imaging experiments were performed essentially as previously described [40]. Further experimental details and information on strains used and statistical analyses are provided in [Supplemental Experimental Procedures](#).

Supplemental Information

Supplemental Information includes Supplemental Experimental Procedures and four figures and can be found with this article online at [doi:10.1016/j.cub.2011.01.053](https://doi.org/10.1016/j.cub.2011.01.053).

Acknowledgments

We are grateful to Rinho Kim, Kyuhung Kim, Sarah Hall, and Ronen Kopito for experimental assistance, Eric Allard for advice on statistical analyses, David Biron and Miriam Goodman for insights and advice, and Miriam Goodman for sharing unpublished data and reagents. We thank Cori Bargmann, Chris Fang-Yen, Chris Gabel, Miriam Goodman, and members of the P.S. lab for comments on the manuscript. This work was funded by the NIH (F31 NS060584 to S.M.W., R01 GM081639 to P.S., core grant P30 NS45713 to the Brandeis Biology Department) and the NSF (IGERT training grant DGE-0549390 to M.B.).

Received: December 1, 2010

Revised: January 20, 2011

Accepted: January 21, 2011

Published online: February 10, 2011

References

- Schepers, R.J., and Ringkamp, M. (2009). Thermoreceptors and thermosensitive afferents. *Neurosci. Biobehav. Rev.* 33, 205–212.
- Dunn, F.A., and Rieke, F. (2006). The impact of photoreceptor noise on retinal gain controls. *Curr. Opin. Neurobiol.* 16, 363–370.
- Shapley, R. (1997). Retinal physiology: Adapting to the changing scene. *Curr. Biol.* 7, R421–R423.
- Grothe, B., and Klump, G.M. (2000). Temporal processing in sensory systems. *Curr. Opin. Neurobiol.* 10, 467–473.
- Maler, L. (2007). Neural strategies for optimal processing of sensory signals. *Prog. Brain Res.* 165, 135–154.
- Hedgecock, E.M., and Russell, R.L. (1975). Normal and mutant thermotaxis in the nematode *Caenorhabditis elegans*. *Proc. Natl. Acad. Sci. USA* 72, 4061–4065.
- Mori, I., and Ohshima, Y. (1995). Neural regulation of thermotaxis in *Caenorhabditis elegans*. *Nature* 376, 344–348.
- Luo, L., Clark, D.A., Biron, D., Mahadevan, L., and Samuel, A.D. (2006). Sensorimotor control during isothermal tracking in *Caenorhabditis elegans*. *J. Exp. Biol.* 209, 4652–4662.

9. Ryu, W.S., and Samuel, A.D. (2002). Thermotaxis in *Caenorhabditis elegans* analyzed by measuring responses to defined Thermal stimuli. *J. Neurosci.* *22*, 5727–5733.
10. Biron, D., Shibuya, M., Gabel, C., Wasserman, S.M., Clark, D.A., Brown, A., Sengupta, P., and Samuel, A.D. (2006). A diacylglycerol kinase modulates long-term thermotactic behavioral plasticity in *C. elegans*. *Nat. Neurosci.* *9*, 1499–1505.
11. Chung, S.H., Clark, D.A., Gabel, C.V., Mazur, E., and Samuel, A.D. (2006). The role of the AFD neuron in *C. elegans* thermotaxis analyzed using femtosecond laser ablation. *BMC Neurosci.* *7*, 30.
12. Clark, D.A., Biron, D., Sengupta, P., and Samuel, A.D.T. (2006). The AFD sensory neurons encode multiple functions underlying thermotactic behavior in *Caenorhabditis elegans*. *J. Neurosci.* *26*, 7444–7451.
13. Kimura, K.D., Miyawaki, A., Matsumoto, K., and Mori, I. (2004). The *C. elegans* thermosensory neuron AFD responds to warming. *Curr. Biol.* *14*, 1291–1295.
14. Clark, D.A., Gabel, C.V., Gabel, H., and Samuel, A.D. (2007). Temporal activity patterns in thermosensory neurons of freely moving *Caenorhabditis elegans* encode spatial thermal gradients. *J. Neurosci.* *27*, 6083–6090.
15. Ramot, D., MacInnis, B.L., and Goodman, M.B. (2008). Bidirectional temperature-sensing by a single thermosensory neuron in *C. elegans*. *Nat. Neurosci.* *11*, 908–915.
16. Inada, H., Ito, H., Satterlee, J., Sengupta, P., Matsumoto, K., and Mori, I. (2006). Identification of guanylyl cyclases that function in thermosensory neurons of *Caenorhabditis elegans*. *Genetics* *172*, 2239–2252.
17. Yu, S., Avery, L., Baude, E., and Garbers, D.L. (1997). Guanylyl cyclase expression in specific sensory neurons: A new family of chemosensory receptors. *Proc. Natl. Acad. Sci. USA* *94*, 3384–3387.
18. Ortiz, C.O., Etchberger, J.F., Posy, S.L., Frøkjær-Jensen, C., Lockery, S., Honig, B., and Hobert, O. (2006). Searching for neuronal left/right asymmetry: Genomewide analysis of nematode receptor-type guanylyl cyclases. *Genetics* *173*, 131–149.
19. Stephens, G.J., Johnson-Kerner, B., Bialek, W., and Ryu, W.S. (2008). Dimensionality and dynamics in the behavior of *C. elegans*. *PLoS Comput. Biol.* *4*, e1000028.
20. Nakai, J., Ohkura, M., and Imoto, K. (2001). A high signal-to-noise Ca(2+) probe composed of a single green fluorescent protein. *Nat. Biotechnol.* *19*, 137–141.
21. Nagai, T., Yamada, S., Tominaga, T., Ichikawa, M., and Miyawaki, A. (2004). Expanded dynamic range of fluorescent indicators for Ca(2+) by circularly permuted yellow fluorescent proteins. *Proc. Natl. Acad. Sci. USA* *101*, 10554–10559.
22. Fitzpatrick, D.A., O'Halloran, D.M., and Burnell, A.M. (2006). Multiple lineage specific expansions within the guanylyl cyclase gene family. *BMC Evol. Biol.* *6*, 26.
23. Murphy, C.T., McCarroll, S.A., Bargmann, C.I., Fraser, A., Kamath, R.S., Ahringer, J., Li, H., and Kenyon, C. (2003). Genes that act downstream of DAF-16 to influence the lifespan of *Caenorhabditis elegans*. *Nature* *424*, 277–283.
24. Hamilton, B., Dong, Y., Shindo, M., Liu, W., Odell, I., Ruvkun, G., and Lee, S.S. (2005). A systematic RNAi screen for longevity genes in *C. elegans*. *Genes Dev.* *19*, 1544–1555.
25. Prahlad, V., Cornelius, T., and Morimoto, R.I. (2008). Regulation of the cellular heat shock response in *Caenorhabditis elegans* by thermosensory neurons. *Science* *320*, 811–814.
26. Ortiz, C.O., Faumont, S., Takayama, J., Ahmed, H.K., Goldsmith, A.D., Pocock, R., McCormick, K.E., Kunimoto, H., Iino, Y., Lockery, S., and Hobert, O. (2009). Lateralized gustatory behavior of *C. elegans* is controlled by specific receptor-type guanylyl cyclases. *Curr. Biol.* *19*, 996–1004.
27. Baude, E.J., Arora, V.K., Yu, S., Garbers, D.L., and Wedel, B.J. (1997). The cloning of a *Caenorhabditis elegans* guanylyl cyclase and the construction of a ligand-sensitive mammalian/nematode chimeric receptor. *J. Biol. Chem.* *272*, 16035–16039.
28. Potter, L.R., and Garbers, D.L. (1992). Dephosphorylation of the guanylyl cyclase-A receptor causes desensitization. *J. Biol. Chem.* *267*, 14531–14534.
29. Potter, L.R., and Hunter, T. (1998). Phosphorylation of the kinase homology domain is essential for activation of the A-type natriuretic peptide receptor. *Mol. Cell. Biol.* *18*, 2164–2172.
30. Trudeau, M.C., and Zagotta, W.N. (2003). Calcium/calmodulin modulation of olfactory and rod cyclic nucleotide-gated ion channels. *J. Biol. Chem.* *278*, 18705–18708.
31. Chen, T.Y., and Yau, K.W. (1994). Direct modulation by Ca(2+)-calmodulin of cyclic nucleotide-activated channel of rat olfactory receptor neurons. *Nature* *368*, 545–548.
32. Spehr, M., Wetzel, C.H., Hatt, H., and Ache, B.W. (2002). 3-phosphoinositides modulate cyclic nucleotide signaling in olfactory receptor neurons. *Neuron* *33*, 731–739.
33. Womack, K.B., Gordon, S.E., He, F., Wensel, T.G., Lu, C.C., and Hilgemann, D.W. (2000). Do phosphatidylinositides modulate vertebrate phototransduction? *J. Neurosci.* *20*, 2792–2799.
34. Bradley, J., Bönigk, W., Yau, K.W., and Frings, S. (2004). Calmodulin permanently associates with rat olfactory CNG channels under native conditions. *Nat. Neurosci.* *7*, 705–710.
35. Krajewski, J.L., Luetje, C.W., and Kramer, R.H. (2003). Tyrosine phosphorylation of rod cyclic nucleotide-gated channels switches off Ca2+/calmodulin inhibition. *J. Neurosci.* *23*, 10100–10106.
36. Satterlee, J.S., Ryu, W.S., and Sengupta, P. (2004). The CMK-1 CaMKI and the TAX-4 cyclic nucleotide-gated channel regulate thermosensory neuron gene expression and function in *C. elegans*. *Curr. Biol.* *14*, 62–68.
37. Robinson, B.L., and McAlpine, D. (2009). Gain control mechanisms in the auditory pathway. *Curr. Opin. Neurobiol.* *19*, 402–407.
38. Shapley, R., and Enroth-Cugell, C. (1984). Visual adaptation and retinal gain controls. *Prog. Retinal Res.* *3*, 263–346.
39. Kuhara, A., Okumura, M., Kimata, T., Tanizawa, Y., Takano, R., Kimura, K.D., Inada, H., Matsumoto, K., and Mori, I. (2008). Temperature sensing by an olfactory neuron in a circuit controlling behavior of *C. elegans*. *Science* *320*, 803–807.
40. Biron, D., Wasserman, S.M., Thomas, J.H., Samuel, A.D., and Sengupta, P. (2008). An olfactory neuron responds stochastically to temperature and modulates *Caenorhabditis elegans* thermotactic behavior. *Proc. Natl. Acad. Sci. USA* *105*, 11002–11007.
41. Kelly, W.G., Xu, S., Montgomery, M.K., and Fire, A. (1997). Distinct requirements for somatic and germline expression of a generally expressed *Caenorhabditis elegans* gene. *Genetics* *146*, 227–238.